Fatigue analysis of a UHPFRC-OSD composite bridge deck for hotspot area strain distributions based on global/local FEM considering crack bridging and interface bond degradations

Hokkaido University ○ Student Member Yuma TAKEUCHI
Central South University Pengru DENG
Hokkaido University Member Takashi MATSUMOTO

1. INTRODUCTION

An orthotropic steel bridge deck (OSD) is widely used for long-span bridges. It is known that the welded connection areas between transverse ribs and a steel bridge deck, i.e., hotspot areas, are susceptible to fatigue. Therefore, in order to assess and enhance the load capacity, it is essential to investigate the behaviors of hotspot areas as well as the development of rehabilitation methods that can improve the fatigue performance of OSD members. One of the rehabilitation methods is overlaying Ultra-High Performance Fiber Reinforced Concrete, i.e., UHPFRC, on the top surface of an OSD, exploiting its advantages, e.g., high strength under both tension and compression.

Hotspot areas are identified as singularities, and about 1mm mesh size is required for accurately calculating the hotspot strains from the finite element method (FEM) [1]. However, it is almost impossible to model and analyze a large-scale structure, e.g., an OSD, with such an extremely refined mesh for local areas. Therefore, the global/local FEM technique is employed in this study. Furthermore, the effect of bond stiffness degradation at the UHPFRC/steel interface on strain results was found to be more predominant than other factors [2].

Therefore, this study aims to investigate the strain distributions in hotspot areas of a UHPFRC-OSD composite bridge deck under fatigue loading based on the global/local FEM, considering the interface bond stiffness degradation as a primary factor in addition to the bridging stress degradation of the UHPFRC overlay.

2. METHOD

In this study, the global/local FEA is carried out using the software MSC/Marc. The analytical model is about a UHPFRC-OSD composite bridge deck, which was tested under a moving wheel load with rubber tires at Civil Engineering Research Institute (CERI) for Cold Region, Hokkaido.

2.1 Material properties

2.1.1 Steel

The material behaviors of steel are represented by a bilinear isotropic hardening stress-strain relation and a von Mises yield criterion. The Poisson's ratio and Young's modulus are given as 0.3 and 200 GPa, respectively. The yield strength of 365 MPa and the ultimate strength of 490 MPa are used in this analysis.

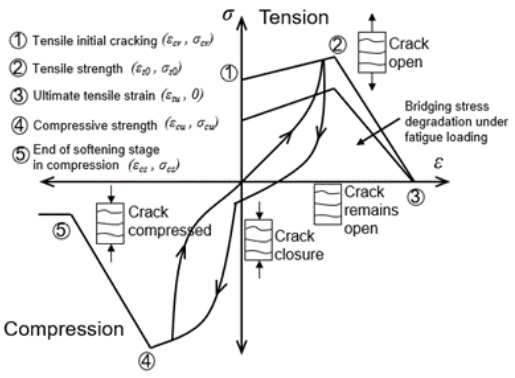

Figure 1 Constitutive law of the cracked UHPFRC component

Table 1 Material properties for UHPFRC

Point	Material properties		Values (unit)
①	Tensile initial cracking	σ_{cr}	6 (MPa)
		ε_{cr}	0.00019
②	Tensile strength	σ_{t0}	9 (MPa)
		ε_{t0}	0.00175
③	Ultimate tensile strain	ε_{tu}	0.01200
④	Compressive strength	σ_{cu}	133 (MPa)
		ε_{cu}	0.00850
⑤	End of softening stage in compression	σ_{cs}	$0.2\sigma_{cu}$
		ε_{cs}	$1.5\ \varepsilon_{cu}$

2.1.2 UHPFRC

The constitutive law and behavior of the cracked UHPFRC are defined in a material user subroutine written in the programming language FORTRAN. The cracking behavior is decomposed into non-cracked and cracked component. The non-cracked component is represented by a linear elastic-isotropic relationship. The Poisson's ratio and Young's modulus are given as 0.22 and 31.3 GPa, respectively. The material properties for the cracked component of UHPFRC are shown and listed in **Figure 1** and **Table 1**.

2.2 Geometry and boundary conditions

In this study, fatigue analyses are carried out based on the global/local FEM. Correspondingly, dimensions, mesh size and boundary conditions are different depending on each model.

2.2.1 Global model

The geometry and boundary conditions of the UHPFRC-OSD composite bridge deck, i.e., Global model are shown in **Figure 2**. The bridge deck plate with a dimension of 3300×2720 mm in longitudinal and transverse direction, respectively, is stiffened by seven longitudinal open bulb ribs and three

transverse cross beams and overlaid by a layer of UHPFRC with the thickness of 25 mm. All elements are modeled as 3-D solid elements with 8 nodes. Global model excludes welds in hotspot areas. Basically, the mesh is appropriate for analyses aiming at global behaviors but is not fine enough for the strains of hotspot areas. In the analysis, a non-uniformly distributed load moving from Center to West to East to Center, i.e., 13 load cases in total with a level of 100kN, is applied as shown in **Figure 2**. The loading starts at the center location. These elements are then unloaded after reaching the peak value, simultaneously with the loading process of the adjacent elements with the same rate for increasing. The procedure is continuously applied along the loading lanes, reproducing the moving process of the wheel load.

2.2.2 Local model

The geometry and boundary conditions of Local model are shown in **Figure 3**. Local model is identical to an area around a hotspot of Global model in dimensions but have welds and different mesh sizes. As shown in **Figure 3** (c), the displacements obtained from Global analysis are applied as boundary conditions to the nodes at the boundary with Global model, which means that the stiffness provided by the adjacent parts of Local model is implicitly considered. It is noted that the region of a local model should be considered carefully when adding new elements, because some boundaries, which a global model does not have, appear and no displacement boundary condition is available for those boundaries. Correspondingly, the accuracy of a local analysis could be worse if the effect of uncoupled boundary conditions is large. In this study, hotspot areas exist near transverse cross beams where relatively large deformation occurs. Because the deformation and welds with the uncoupled boundary conditions accelerate the unreasonable strain behaviors of hotspot areas, small areas are chosen for Local model to exclude deformations of the deck plate near the transverse cross beams and only include those near the scallops. First, the area around the hotspot is cut out, as shown in **Figure 3** (a) and (b). Then, to meet the required mesh size and make more detailed dimensions, Local model is divided into five and welds with a 10 mm triangle shape are added as a steel model, as shown in **Figure 3** (c). The material properties and element types are the same as those in Global model. **Figure 3** (b) also shows the locations of a hotspot and strain gauges installed in the experiment following the 1-point representative or 3-point extrapolation method. In this study, the vertical strain on the y-axis is investigated at the strain gauge installation points of the hotspot areas for each cycle of fatigue analysis.

2.3 Degradation model

2.3.1 Bridging stress degradation of cracked UHPFRC

Under fatigue loadings, the reduction in bridging stress between crack surfaces is considered in the analytical model to reproduce the fatigue deterioration. The bridging stress degradation is expressed as a function of the maximum tensile strain ε_{tmax} and the number of cycles N. The employed

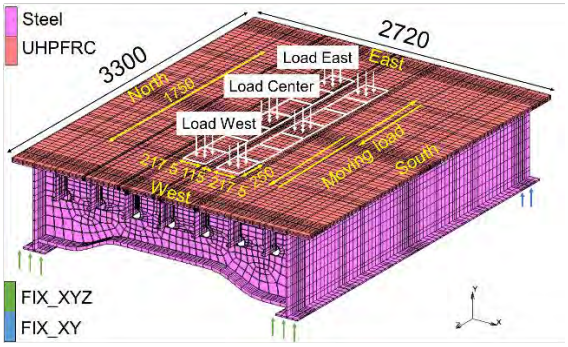

Figure 2 Dimensions and boundary conditions of the composite bridge deck, i.e., Global model (unit: mm)

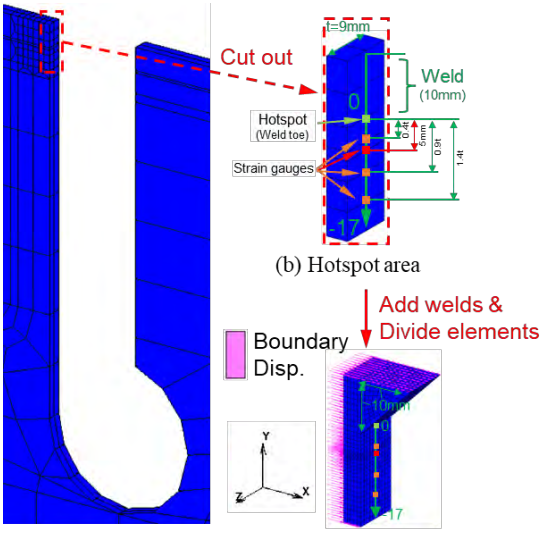

(b) Hotspot area

(a) Scallop of Global model (c)Local model

Figure 3 Dimensions and boundary conditions of Local model (unit: mm)

bridging stress degradation model of UHPFRC is expressed by

$$\frac{\sigma_N}{\sigma_1} = f(\varepsilon_{tmax}, N) \leq 1 \quad (1)$$

$$\frac{\sigma_N}{\sigma_1} = 1 - (a_0 + a_1 \varepsilon_{tmax}) \log N \quad (2)$$

where σ_N/σ_1 is the bridging stress degradation ratio between the Nth and the first cycle. a_0 and a_1 are the degradation coefficients, chosen as 0.015 and 5, respectively, for UHPFRC material [3].

2.3.2 Bond degradation at the UHPFRC/steel interface

For the current UHPFRC-OSD composite bridge deck, epoxy resin is employed to bond UHPFRC to a steel substrate, which can provide a connection to avoid stress concentration. However, debonding at the UHPFRC/steel interface can occur even during early cycles, affecting the fatigue behaviors of the hotspot areas significantly.

Although there are several types of debonding failures, the normal tensile and shear failure modes at the Epoxy/UHPFRC interface are the main causes of epoxy adhesive debonding at the UHPFRC/steel interface [4]. It was reported that the tangential shear and normal tensile strengths of the interface are 5.14 MPa and 1.18 MPa, respectively, from direct shear and

tensile tests. Therefore, once the stress reaches these values at the bottom of the UHPFRC layer in each direction, the region is considered a debonding area for the following cycles.

By applying the GLUED and TOUCHING options in MSC/Marc, the interfacial bonding and debonding models between the UHPFRC overlay and the steel plate are represented. For the bonding property, the GLUED option is used to describe a linear elastic relationship with the elastic modulus, which is 2.66 GPa in both normal and tangential directions. Meanwhile, for the debonding property, the TOUCHING option is used. Before proceeding to the next cycle, the debonding area is confirmed based on the above-mentioned relative relationship between interfacial stresses and bond strengths and then applied in the subsequent cycle analysis.

3. RESULTS AND DISCUSSIONS

3.1 Results of below 10000th cycles under fatigue loading

In this chapter, the strain behaviors affected by debonding at below 10000th cycles of fatigue loading are explained.

3.1.1 Normal tensile stress distribution

Normal tensile strength is comparatively smaller than shear strength. Therefore, debonding is mainly attributed to tensile stresses caused by wheel loadings at the UHPFRC bottom layer. **Figure 4** shows the normal tensile stress distribution of the UHPFRC bottom layer at the 1st, 1000th, and 10000th cycles under Load Center. As shown in this figure, gray-colored areas where the stresses are greater than the normal tensile strength are considered debonding areas in the following cycles. At early fatigue loading cycles, debonding is observed even in local regions around hotspot areas, apart from loading lanes. This may occur due to not only wheel loadings but also geometry changes caused by scallops that exist under the layer. Furthermore, it is discovered that, with the exception of the areas under the loading lanes, the debonding areas around hotspots do not expand as the loading cycle increases. Besides, it is recognized that the direction and magnitude of stress at hotspot areas change due to the debonding, and strain behaviors may be affected accordingly.

3.1.2 Strain distribution of hotspot areas

As mentioned in the previous section, due to the debonding at early cycles, the strain in hotspot areas may change accordingly. **Figure 5** shows the result of the strain distribution in the second hotspot area from the north, i.e., the hotspot area apart from loading lanes, at early cycles. The red dotted and solid lines show the results of only Global analysis and Global/Local analysis at the 1st cycle, respectively. As shown in the figure, using Global/Local analysis, which allows for fine mesh and detailed weld shape, improves analytical accuracy as the result moves from red dotted to solid lines. On the contrary, the blue and orange lines show the results of the 1000th and 10000th cycles, respectively, in **Figure 5**. There is a tendency for strain to decrease at early cycles in the experiment, and it is found that the trend can be reproduced by incorporating the setting of

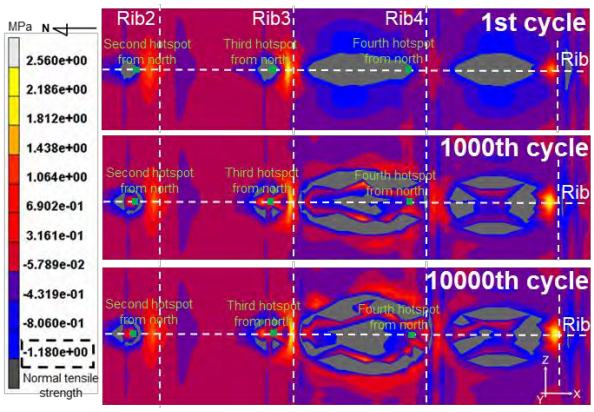

Figure 4 Normal tensile stress distribution of the UHPFRC bottom layer under Load Center

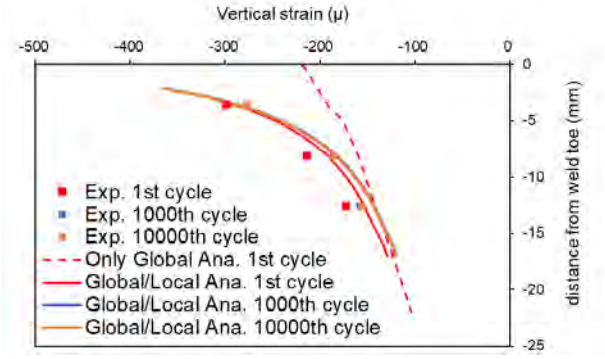

Figure 5 Strain distribution in the second hotspot area from the north, i.e., the hotspot area apart from loading lanes

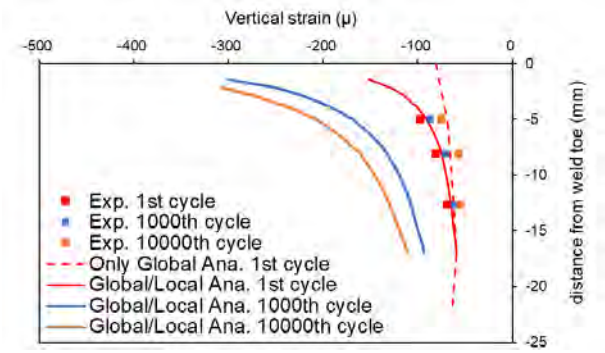

Figure 6 Strain distribution in the fourth hotspot area from the north, i.e., the hotspot area under loading lanes

debonding locally because the result moves from the red to the blue and orange lines. On the other hand, **Figure 6** shows the result of the strain distribution in the fourth hotspot area from the north, i.e., the hotspot area under loading lanes. As shown in the figure, the analytical result of the strain behaviors in the fourth hotspot area from the north does not match the experimental ones, although there is a locally occurring debonding around the scallop, similar to that in the second hotspot area from the north. This phenomenon may happen due to the difference in size of the debonding areas between the hotspot areas apart from and under loading lanes. As shown in **Figure 4**, the second hotspot area from the north only has small debonding regions at the 1st cycle compared to the area under

loading lanes. On the contrary, the fourth hotspot area has such large debonding regions because the location is under loading lanes. Then, the strain becomes larger, as the loading cycle increases and the debonding area is expanded correspondingly. However, in practice, debonding may not be as extensive because it could be restrained by the middle transverse cross beam and not occur even if the stresses are greater than the normal tensile strength. The current method determines debonding areas while ignoring the effect of supportive components, e.g., the middle transverse crossbeam, on debonding. Therefore, it is concluded that debonding happens locally only at the space of the scallop and that the phenomenon causes the strain behaviors of hotspot areas to be smaller. With too many debonding areas around hotspots, the accuracy would be worse. In other words, in order to obtain more accurate results, further investigation of contact characteristics, especially for the areas above the ribs, should be carried out, which was not done in this study.

3.2 Results of whole cycles under fatigue loading

As mentioned in the previous chapter, there is no inappropriate debonding area around the second hotspot area from the north, and its strain behaviors are in good agreement with experimental ones at early cycles. **Figure 7** shows the relationships between strain distributions and the number of loading cycles under fatigue loading for a location 3.6 mm away from the weld toe at the second hotspot area from the north, i.e., the hotspot area apart from loading lanes. The orange line shows the result only using the bridging stress degradation for UHPFRC without Global/Local FEM and the interface bond degradation. Compared to the black line, which is an experimental result, the result with only bridging stress degradation is way smaller and worse. In addition, strain does not change even as the loading cycle increases due to the lack of a debonding setting. On the contrary, as shown in **Figure 7**, the accuracy is improved by Global/Local analysis as the result moves from orange to red. Besides, strain gets smaller at early

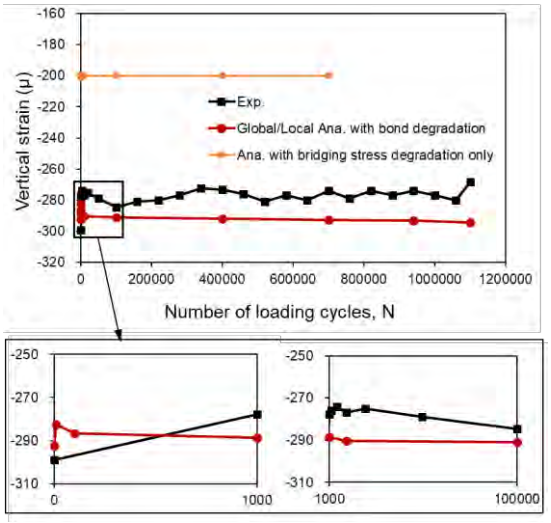

Figure 7 Vertical strain to the number of loading cycles at the location 3.6 mm away from weld toe in the second hotspot area from the north, i.e., the hotspot area apart from loading lanes

cycles, similar to the experimental behavior, due to debonding occurring only in local areas. Afterwards, the experimental strain behavior gets larger again, and the analysis exhibits the same tendency due to the expansion of debonding areas under loading lanes, but the rate is really fast, as shown in the lower magnified ones of **Figure 7**. With more cycles, the experimental strain behaviors decrease slowly but continuously; nevertheless, the analytical result stays almost unchanged. This may be because the bond stiffness and strength of the UHPFRC/steel interface used in this study are not related to the number of loading cycles. Therefore, to more accurately reproduce the fatigue strain behaviors, further experimental investigation of the UHPFRC/steel interfacial fatigue characteristic of the composite bridge deck as well as the effect on debonding of supportive components, e.g., middle transverse cross beams, should be conducted.

4. CONCLUSION

In this study, a 3D non-linear analysis is performed to investigate strain distributions in hotspot areas of a UHPFRC-OSD composite bridge deck under fatigue loading based on the global/local FEM, considering interface bond degradations as a primary factor. It is found that the global/local analysis can improve the analytical accuracy of hotspot areas. And it is discovered and reproduced in the analysis that the locally occurring debonding of the early cycle around the scallops causes a decrease in strain in the early stages of the experiment. After that, the strain gets larger again, corresponding to the debonding expansion in the areas under the loading lanes.

5. FUTURE WORK

Further research on the contact properties should be carried out to examine and employ the fatigue characteristic of epoxy adhesive and the effect on debonding of the supportive components in order to more accurately reproduce the fatigue behaviors of hotspot areas.

ACKNOWLEDGEMENT

The authors gratefully acknowledge the support provided by the J-THIFCOM association.

REFERENCES

1) Takeuchi, Y., Deng, P. and Matsumoto, T.: Global/Local FEA for the strain in the welding areas of steel bridge deck. JSCE Hokkaido branch No. 77, No. A-24, Japan, 2021.
2) Ma, C.H., Deng, P. and Matsumoto, T.: Fatigue analysis of a UHPFRC-OSD composite structure considering crack bridging and interfacial bond stiffness degradations. Engineering Structures, Vol. 249, 113330, 2021.
3) Jimi, H., Deng, P. and Matsumoto, T.: Bridging stress degradation model of UHPFRC from numerically fitting fatigue flexural test results using FEA. JSCE Hokkaido branch No. 77, No. A-46, Japan, 2021.
4) Zou, Y., Jiang, J., Zhou, Z., Wang, X. and Guo, J.: Study on the Static Performance of Prefabricated UHPC-Steel Epoxy Bonding Interface. Hindawi, Advances in Civil Engineering, Vol. 15, 6663517, 2021.